

# Implantation Energy Dependence on Deuterium Retention Behaviors for the Carbon Implanted Tungsten

Yasuhisa Oya<sup>1)\*</sup>, Makoto Kobayashi<sup>1)</sup>, Naoaki Yoshida<sup>2)</sup>, Naoko Ashikawa<sup>3)</sup>, Akio Sagara<sup>3)</sup>, Yuji Hatano<sup>4)</sup>, and Kenji Okuno<sup>1)</sup>

<sup>1)</sup> *Radioscience Research Laboratory, Faculty of Science, Shizuoka University, 836, Ohya, Suruga-ku, Shizuoka 422-8529, Japan.*

<sup>2)</sup> *Institute for Applied Mechanics, Kyushu University, Fukuoka 816-8580, Japan.*

<sup>3)</sup> *National Institute for Fusion Science, Gifu 509-5292, Japan.*

<sup>4)</sup> *Hydrogen Isotope Research Center, University of Toyama, 3190, Gofuku, Toyama 930-8555, Japan.*

(Received: 9 May 2012 / Accepted: 8 August 2012)

Effects of energetic carbon implantation on deuterium retention behavior in tungsten were studied. The dislocation loops and vacancies were introduced in tungsten as irradiation damages by energetic carbon implantation. The density of irradiation damages was almost saturated by C<sup>+</sup> implantation below 1 dpa according to TEM observations. The retentions of deuterium trapped by dislocation loops and vacancies were observed in TDS measurements, which were increased as increasing the carbon implantation energy. The deuterium desorption at higher temperature above 600 K was also found, corresponding to the desorption of deuterium retained in the intrinsic cavity in bulk region. However, this trapping was refrained by energetic C<sup>+</sup> implantation, concluding that the retained carbon would play a role as the diffusion barrier of deuterium, which would prevent deuterium penetration through bulk.

Keywords: Tungsten, TDS, TEM, Carbon, Irradiation damage, Diffusion, Simultaneous implantation

## 1. Introduction

Tungsten is a candidate for plasma facing materials (PFMs) in fusion devices due to its low hydrogen solubility, low sputtering yield and high melting point [1]. The usage of carbon fiber composite (CFC) is also considered in the high heat load region of divertor in fusion reactor, because of its high melting point [2]. These materials will be exposed to energetic particles from plasma during reactor operation. It is well known that carbon materials are easily eroded by energetic hydrogen isotopes by chemical or physical sputtering processes. Then, sputtered carbon will be implanted into tungsten with hydrogen isotopes during plasma operation, which will form the tungsten-carbon (W-C) mixed layer on the surface region of tungsten [3-5]. Hydrogen isotopes including tritium will be implanted simultaneously with formation of W-C mixed layer, and will dynamically interact with carbon in tungsten. In the view point of the fuel recycling, it is important to elucidate the retention behavior of hydrogen isotopes retained on tungsten materials in the fusion environment.

In our previous studies, deuterium retention behavior in tungsten with simultaneous 10 keV C<sup>+</sup> implantation was evaluated. Enhancement of deuterium retention by the

introduction of irradiation damages was clearly observed because 10 keV C<sup>+</sup> implantation induced higher displacement damage in tungsten than that by deuterium [6]. On the other hand, it is reported that the carbon retained in tungsten plays a role of diffusion barrier for hydrogen isotopes toward the bulk, resulting in the decrease of hydrogen isotope retention in tungsten [7]. Recent ion-driven permeation experiments under carbon - deuterium simultaneous implantation indicate that deuterium permeation is promoted by simultaneous carbon implanted tungsten [8, 9]. These results indicate the estimation of hydrogen isotope retention in tungsten is complicated under fusion environment. Therefore, deuterium retention in tungsten implanted with carbon was investigated in this study to understand the effect of carbon implantation on deuterium retention behavior in tungsten. For this objective, two types of implantation were carried out. One was the simultaneous implantation (C<sup>+</sup> - D<sub>2</sub><sup>+</sup> sim. imp.) where carbon and deuterium were implanted into tungsten simultaneously. In the simultaneous implantation circumstance, deuterium was retained in tungsten with formations of irradiation defects and W-C mixed layer. The other implantation was the sequential implantation (C<sup>+</sup> - D<sub>2</sub><sup>+</sup> seq. imp.), meaning that

author's e-mail: syoya@ipc.shizuoka.ac.jp

carbon was implanted into tungsten prior to deuterium. In the sequential implantation, deuterium was implanted into tungsten after formations of irradiation defects and W-C mixed layer. In addition, implantation energy of carbon was changed to investigate dependences of the distribution of carbon and damage on deuterium retention behavior. The deuterium retentions were evaluated by means of Thermal Desorption Spectroscopy (TDS) measurements. The irradiation damages were also observed by Transmission Electron Microscopy (TEM) at Kyushu University.

## 2. Experimental

A disk-type polycrystalline tungsten with stress-relieved conditions (heated at 1173 K), which was supplied by Allied Material Co. Ltd was used. The sample size was 10 mm diameter and 0.5 mm thickness. The Sample was polished mechanically to the roughness of less than 1  $\mu\text{m}$  by SiC abrasive papers and mono-crystalline diamond suspensions, and preheated at 1173 K for 30 minutes under ultrahigh vacuum to remove the impurities and damages introduced during the polishing processes. Then, simultaneous or sequential carbon ion ( $\text{C}^+$ ) and deuterium ion ( $\text{D}_2^+$ ) implantations were performed in the  $\text{C}^+$ - $\text{D}_2^+$  simultaneous implantation apparatus at room temperature. In this apparatus, the sample can be irradiated independently by two different ion guns, namely  $\text{C}^+$  and  $\text{D}_2^+$  guns. In the  $\text{C}^+$  gun,  $\text{CO}_2$  was used as the  $\text{C}^+$  source gas to get rid of hydrogen impurities. The  $E \times B$  mass separator was equipped at the head of the  $\text{C}^+$  gun to extract pure  $\text{C}^+$ . The incident angles for the  $\text{C}^+$  and  $\text{D}_2^+$  guns were 15 degrees from the sample surface normal, forming an angle of 30 degrees between the two beams. The energy of  $\text{C}^+$  was changed from 5 to 10 keV and that of  $\text{D}_2^+$  was set to be 2 - 3 keV. The  $\text{C}^+$  and  $\text{D}^+$  flux were  $0.1 \times 10^{18} \text{ C}^+ \text{ m}^{-2} \text{ s}^{-1}$  and  $1.0 \times 10^{18} \text{ D}^+ \text{ m}^{-2} \text{ s}^{-1}$ , respectively. Therefore, for  $\text{C}^+$ - $\text{D}_2^+$  simultaneous implantation, the ion flux ratio was set to be  $\text{C}^+/\text{D}^+ = 0.1$ . The  $\text{C}^+$  fluence was constant to be  $0.1 \times 10^{22} \text{ C}^+ \text{ m}^{-2}$  in  $\text{C}^+$ - $\text{D}_2^+$  sequential implantation.  $\text{D}^+$  fluence was changed in the range of  $(0.1 - 1.8) \times 10^{22} \text{ D}^+ \text{ m}^{-2}$ . The only  $\text{D}_2^+$  implantation was also performed to compare the deuterium retention in  $\text{C}^+$  implanted tungsten. The chemical states of carbon and tungsten were studied by X-ray Photoelectron Spectroscopy (XPS). The TDS measurements were performed from room temperature to 1173 K with a heating rate of  $0.5 \text{ K s}^{-1}$ . The TEM observations were also performed to investigate the irradiation damages formed by the ion implantations. The depth profile of deuterium was analyzed by Glow Discharge Optical Emission Spectroscopy (GD-OES).

## 3. Results and discussion

Fig. 1 show TEM images of tungsten implanted by 3

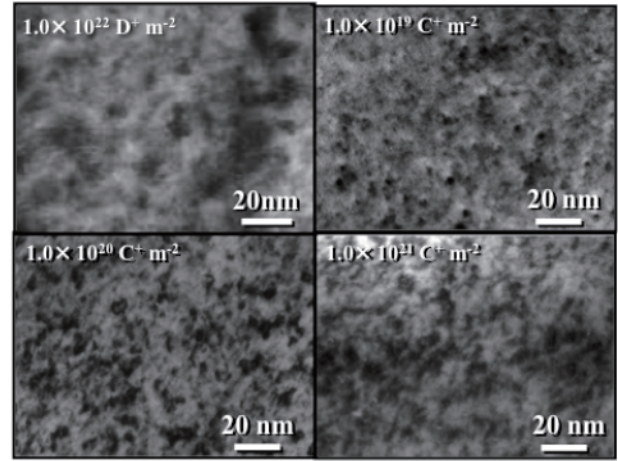


Fig. 1 TEM images of tungsten implanted with 3 keV  $\text{D}_2^+$  or 10 keV  $\text{C}^+$  at various ion fluences.

keV  $\text{D}_2^+$  with the fluence of  $1.0 \times 10^{22} \text{ D}^+ \text{ m}^{-2}$  and tungsten with 10 keV  $\text{C}^+$  with different  $\text{C}^+$  fluences in the range of  $(0.001-0.1) \times 10^{22} \text{ C}^+ \text{ m}^{-2}$ . For all the samples, lots of dislocation loops were introduced in tungsten by ion implantations, which was quite different from pure tungsten where its density was low. In addition, since the irradiation vacancy and dislocation loop are pair defects, the formation of dislocation loops indicated the introduction of vacancies. It was also found that even higher fluence of  $\text{D}^+$ , density of irradiation defects in tungsten with 10 keV  $\text{C}^+$  implantation was higher than that with 3 keV  $\text{D}_2^+$  implantation, indicating that irradiation damages were easily introduced in tungsten by 10 keV  $\text{C}^+$  implantation compared to that by 3 keV  $\text{D}_2^+$  implantation due to higher implantation energy, higher mass and larger atomic radius. It was also found that density of irradiation damages in tungsten induced by 10 keV  $\text{C}^+$  implantation was increased in the  $\text{C}^+$  fluence range of  $(0.001-0.01) \times 10^{22} \text{ C}^+ \text{ m}^{-2}$ , but its density was seen to be the same with  $\text{C}^+$  fluence larger than  $0.01 \times$

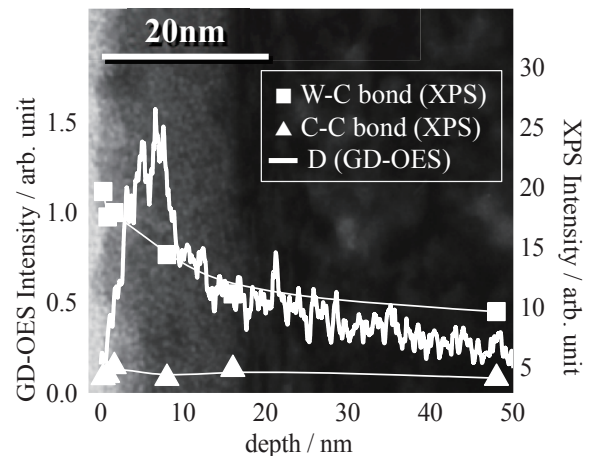


Fig. 2 Depth profiles of D observed by GD-OES and W-C and C-C bonds by XPS. The TEM image was also shown in this figure.

$10^{22} \text{ C}^+ \text{ m}^{-2}$ , indicating that density of irradiation defects were saturated in the  $\text{C}^+$  fluence of  $0.01 \times 10^{22} \text{ C}^+ \text{ m}^{-2}$ . By the SRIM (Stopping range of Ions in Matter) code calculation [10], irradiation defects in tungsten implanted by 10 keV  $\text{C}^+$  with the  $\text{C}^+$  fluence of  $0.01 \times 10^{22} \text{ C}^+ \text{ m}^{-2}$  were distributed within 30 nm beneath the surface, with the peak at around 5 nm (1.3 dpa), indicating that the density of irradiation defects would be saturated below 1.3 dpa. The depth profiles of D observed by GD-OES at University of Toyama and, W-C and C-C bonds evaluated by XPS were shown in Fig. 2. The TEM image was also overlapped in this figure. It was found that most of D was retained in W-C mixed layers and major chemical state of C in this layer was found to be W-C bond.

Fig. 3 shows  $\text{D}_2$  TDS spectra for only 3 keV  $\text{D}_2^+$  implanted tungsten and 10 keV  $\text{C}^+$  - 3 keV  $\text{D}_2^+$  sequentially implanted one with various  $\text{D}^+$  fluences. These spectra were consisted of three desorption stages at around 370, 480 and 620 K which were named as Peaks 1, 2 and 3, respectively. In lower  $\text{D}^+$  fluence of  $0.1 \sim 0.3 \times 10^{22} \text{ D}^+ \text{ m}^{-2}$ , the deuterium retentions as Peaks 1 and 2 were clearly increased by  $\text{C}^+$  implantation, indicating that these desorption stages would be related to the deuterium interacted with the irradiation damages. The density of irradiation damages induced by 10 keV  $\text{C}^+$  implantation was higher than that by 3 keV  $\text{D}_2^+$  implantation as shown in Fig. 1, resulting in the higher deuterium retention for the 10 keV  $\text{C}^+$  implanted tungsten. In general, trapping energy of deuterium by vacancy would be higher than that by dislocation loop [11,12], indicating that Peaks 1 and 2 could be assigned to the desorption stages of deuterium trapped by dislocation loops and vacancies, respectively. In higher fluence of  $1.8 \times 10^{22} \text{ D}^+ \text{ m}^{-2}$ , the deuterium retentions as Peaks 1 and 2 for  $\text{C}^+$  implanted W were almost the same as that without  $\text{C}^+$  implantation, indicating that deuterium trappings by irradiation damages should be almost saturated. However, the deuterium retention as Peak 3 for only  $\text{D}_2^+$  implanted tungsten was higher than that for 10 keV  $\text{C}^+$  - 3 keV  $\text{D}_2^+$  sequentially implanted one. The amount of trapping site as Peak 3 was not induced by ion implantation because the retention of deuterium as Peak 3 was not increased by 10 keV  $\text{C}^+$  implantation. Therefore, the promising trapping site for Peak 3 would be intrinsic sites such as cavities, grain boundary and/or oxygen impurity [13,14]. Lower deuterium retention as Peak 3 for 10 keV  $\text{C}^+$  - 3 keV  $\text{D}_2^+$  sequentially implanted tungsten would indicate that deuterium diffusion in tungsten was refrained by 10 keV  $\text{C}^+$  implantation.

The retentions of deuterium retained as Peaks 1, 2 and 3 for tungsten with 10 keV  $\text{C}^+$  - 3 keV  $\text{D}_2^+$  sequential implantation or simultaneous implantations were compared in Fig. 4. The deuterium retentions for the samples with the  $\text{D}^+$  fluence of  $1.8 \times 10^{22} \text{ D}^+ \text{ m}^{-2}$  were

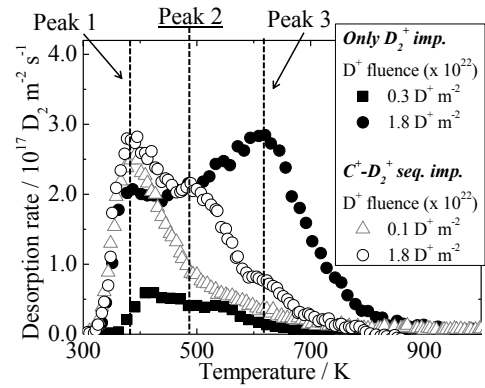


Fig. 3  $\text{D}_2$  TDS spectra of 3 keV  $\text{D}_2^+$  implanted tungsten and 10 keV  $\text{C}^+$  - 3 keV  $\text{D}_2^+$  implanted one.

compared. In the case of  $\text{C}^+$ -  $\text{D}_2^+$  simultaneous implantation, the retention of deuterium retained as Peak 3 was decreased by  $\text{C}^+$  implantation, which was almost the same with both of sequential and simultaneous implantations. However, the deuterium retentions as Peaks 1 and 2 for the simultaneous implantation were increased compared to those for the sequential implantation. The deuterium trappings as Peaks 1 and 2 for  $\text{C}^+$ -  $\text{D}_2^+$  simultaneously implanted tungsten were higher than that for sequentially implanted tungsten, indicating that simultaneous implantation effects were contributed to the increase of deuterium retentions in these peaks.

To clarify the simultaneous implantation effects on deuterium retention behavior in tungsten, incident energy of  $\text{C}^+$  was changed for both of sequential or simultaneous implantations. The implantation energy of  $\text{D}_2^+$  was fixed to be 2 keV. Figs. 5 (a) and (b) show the  $\text{D}_2$  TDS spectra for  $\text{C}^+$  -  $\text{D}_2^+$  simultaneously implanted tungsten and  $\text{C}^+$  -  $\text{D}_2^+$  sequentially implanted one as a function of  $\text{C}^+$  incident energy, respectively. Both of  $\text{D}^+$  and  $\text{C}^+$  fluences were set to be  $1.0 \times 10^{22} \text{ D}^+ \text{ m}^{-2}$  and  $0.1 \times 10^{22} \text{ C}^+ \text{ m}^{-2}$ , respectively. The  $\text{D}_2$  TDS spectra were slightly changed in simultaneous implantation case although little changes

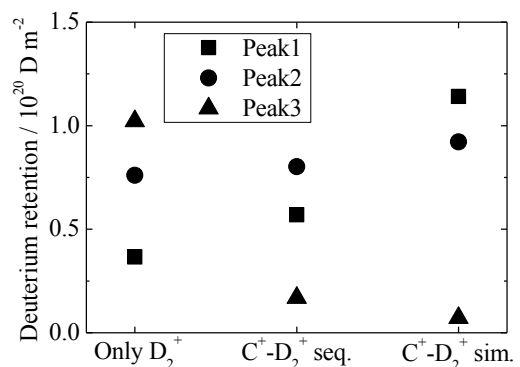


Fig. 4 Comparison of deuterium retentions as Peaks 1, 2 and 3 for tungsten implanted with various implantation procedure.

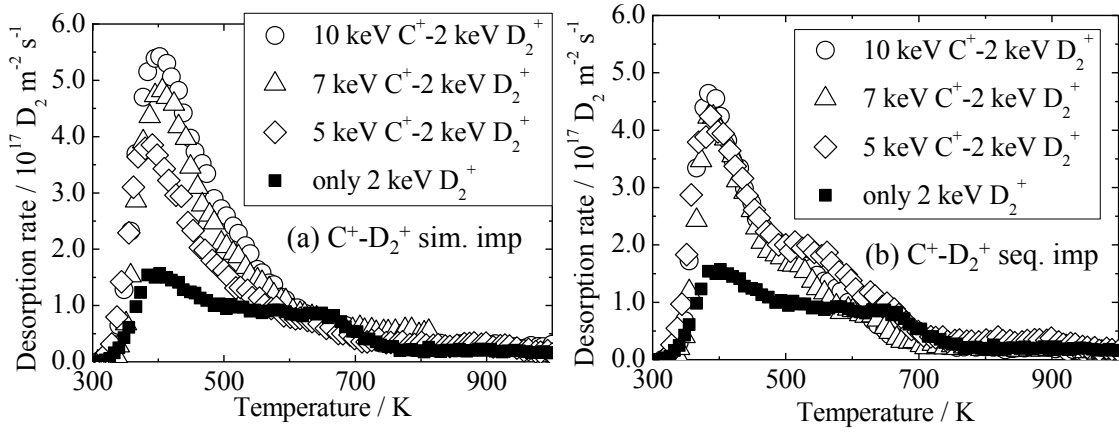


Fig. 5  $D_2$  TDS spectra of tungsten with (a)  $C^+ - 2\text{ keV } D_2^+$  simultaneous and (b)  $C^+ - 2\text{ keV } D_2^+$  sequential implantation with various  $C^+$  incident energies

were observed in that for  $C^+ - D_2^+$  sequentially implanted tungsten. Fig. 6 summarizes the retentions of deuterium retained as Peaks 1, 2 and 3. The deuterium retention as Peak 1 was clearly increased for  $C^+ - D_2^+$  simultaneously implanted tungsten. It was found that the no difference of deuterium retention for  $C^+ - D_2^+$  sequentially implanted tungsten was observed nonetheless  $C^+$  incident energy was changed from 5 to 10 keV. By changing the  $C^+$  incident energies from 5 to 10 keV  $C^+$ , the density of irradiation damages was estimated to be above 10 dpa, indicating that the density of irradiation defects was saturated in all the samples. However, distributions of irradiation defects induced by  $C^+$  implantation were changed with incident energy from SRIM code calculation. With increasing  $C^+$  incident energy, distribution of irradiation damages was expanded toward the depth. The irradiation damages induced by 10 keV  $C^+$  were extended from surface to 30 nm of depth although those by 5 keV  $C^+$  were limited with 20 nm from the surface, indicating that the increase of deuterium retention with increasing  $C^+$  incident energy observed for

the simultaneously implanted tungsten was resulted from distribution of irradiation damages. Deuterium trappings by irradiation defects in deeper region (20 - 30 nm beneath surface) would be contribution to these increases of deuterium retention as Peaks 1 and 2. However in the case of  $C^+ - D_2^+$  sequential implantation, deuterium retention was not increased with increasing  $C^+$  incident energy, considering that retained carbon would prevent deuterium penetration into bulk region. In  $C^+ - D_2^+$  sequential implantation, the 2 keV  $D_2^+$  was implanted into tungsten after  $C^+$  implantation. Therefore, implanted deuterium should be affected by retained carbon in tungsten. On the other hand in  $C^+ - D_2^+$  simultaneous implantation, several portion of deuterium was implanted into tungsten before retaining carbon enough to prevent deuterium diffusion into bulk.

In summary, the retention of deuterium trapped by irradiation damages was enhanced by energetic carbon implantation. The deuterium retention by intrinsic cavity in bulk region was also found and was decreased by energetic carbon implantation. Therefore, it was

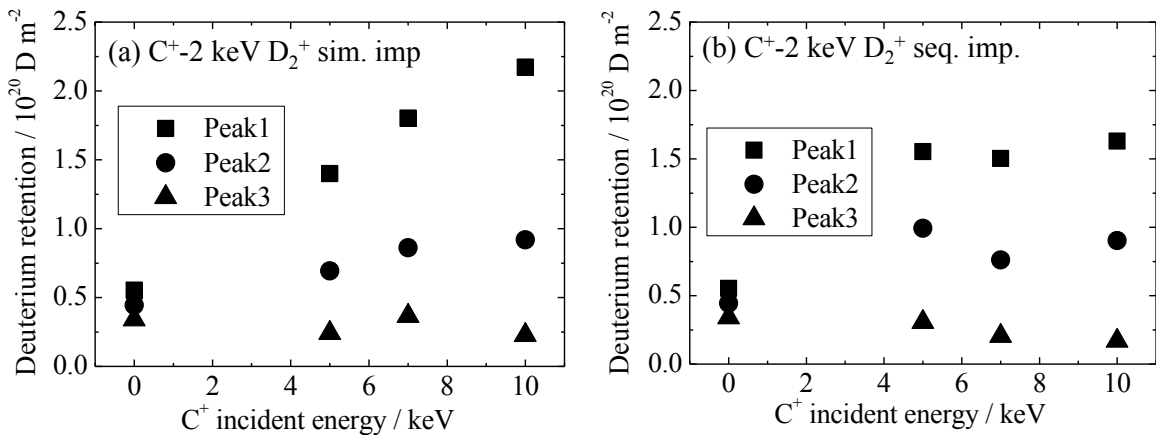


Fig. 6 Deuterium retention for each peak of tungsten with (a)  $C^+ - D_2^+$  simultaneous and (b)  $C^+ - D_2^+$  sequential implantation with various  $C^+$  incident energies.



considered that implanted carbon would play a role as the deuterium diffusion barrier leading the reduction of deuterium penetration toward the bulk. However, several experiments showed deuterium ion-driven permeation was promoted by carbon simultaneously implanted into tungsten. These facts can be explained by the project range of carbon and deuterium ions. In our experiments, the project range of 5 - 10 keV C<sup>+</sup> were almost the same as that of 2 - 3 keV D<sub>2</sub><sup>+</sup>. As the project range of carbon reported in ref. [8,9] was shorter than that of deuterium, higher portion of deuterium was implanted deeper region of tungsten than carbon. The implanted deuterium was easily permeated through tungsten because of the decreased diffusivity in the implanted surface by carbon.

#### 4. Conclusions

The effects of energetic carbon implantation on deuterium retention behavior in tungsten were investigated in this study. Dislocation loops and vacancies were formed in tungsten as irradiation defects by energetic carbon implantation. The density of irradiation damage was saturated below about 1 dpa by TEM observations. Deuterium retentions by dislocation loops and vacancies were observed in TDS measurements. Deuterium retentions by irradiation defects were increased by energetic carbon implantation. Deuterium retention by intrinsic cavity in bulk region was also found and was decreased by energetic carbon implantation. It was concluded that retained carbon would play a role as the diffusion barrier of deuterium, preventing deuterium to penetrating into bulk.

#### Acknowledgement

This study was supported by JSPS Kakenhi No. 22360389, NIFS collaboration program NIFS11KEMF022, University of Toyama collaboration program and the Center for Instrumental Analysis at Shizuoka University.

#### References

- [1] R. P. Doerner *et al.*, *J. Nucl. Mater.* **363-365**, 32-40 (2007).
- [2] S. Pestchanyi *et al.*, *Fusion Eng. Des.* **66-68**, 271-276 (2003).
- [3] I. Bizyukov, *et al.*, *J. Nucl. Mater.*, **363-365**, 1184-1189 (2007).
- [4] V. Kh. Alimov, *Phys. Scr.*, **T108**, 46-56 (2004).
- [5] H.T. Lee, *et al.*, *J. Nucl. Mater.* **390-391**, 971-974 (2009).
- [6] M. Kobayashi, *et al.*, *Phys. Scr.* **T138**, 014050 (2009).
- [7] V. Kh. Alimov, *et al.*, *J. Nucl. Mater.*, **375**, 192 (2008).
- [8] Y. Ueda *et al.*, *J. Nucl. Mater.*, 2012 in press.
- [9] H. Y. Peng *et al.*, *Phys. Scr.* **T145**, 014046 (2011).
- [10] J.F. Ziegler, 2006 SRIM code.
- [11] M. Poon *et al.*, *J. Nucl. Mater.*, **374**, 390 (2008).
- [12] J. Roth and K. Schmid *Phys. Scr.* **T145**, 014031 (2011).
- [13] V.Kh. Alimov *et al.*, *J. Nucl. Mater.* **337-339**, 619-623

(2005).

- [14] T. Ahlgren *et al.*, *J. Nucl. Mater.* In press.